Stability and convergence of finite element approximation schemes for harmonic maps

Sören Bartels*

Department of Mathematics, Humboldt-Universität zu Berlin, Unter den Linden 6, D-10099 Berlin, Germany. *E-Mail:* sba@math.hu-berlin.de

Abstract. This article discusses stability and convergence of approximation schemes for harmonic maps. A finite element discretization of an iterative algorithm due to F. Alouges is introduced and shown to be stable and convergent in general only on acute type triangulations. An a posteriori criterion is proposed which allows to monitor sufficient conditions for weak convergence to a harmonic map on general triangulations and for adaptive mesh refinement. Numerical experiments show that an adaptive strategy automatically refines triangulations in neighborhoods of typical point singularities and thereby underline its efficiency.

Key Words. Harmonic maps, iterative algorithm, finite element method, weak convergence, liquid crystals, adaptive refinement.

AMS Subject Classification: 35A40, 65C20, 65N30.

Date: March 11, 2005.

1. INTRODUCTION

A variational model in the theory of nematic liquid crystals due to Oseen and Frank [31, 12, 24, 14] leads to a minimization of the energy functional

$$I(v) := \frac{1}{2}\int_\Omega k_1|\operatorname{div} v|^2 + k_2|v\cdot\operatorname{curl} v|^2 + k_3|v\times\operatorname{curl} v|^2 + (k_2+k_4)\big(\operatorname{tr}[(Dv)^2] - (\operatorname{div} v)^2\big)\,\mathrm{d}x$$

over a space of admissible configurations

$$v \in \mathcal{A}(u_{\mathrm{D}}) := \{v \in H^1(\Omega;\mathbb{R}^3) :\, v|_{\partial\Omega} = u_{\mathrm{D}},\, |v| = 1 \text{ a.e. in } \Omega\}.$$

Here, $\Omega \subseteq \mathbb{R}^3$ is a bounded Lipschitz domain and represents the physical domain in which the liquid crystal is embedded, $u_{\mathrm{D}} \in H^{1/2}(\partial\Omega;\mathbb{R}^3)$ with $|u_{\mathrm{D}}| = 1$ almost everywhere on $\partial\Omega$ are given boundary data, and $k_1, k_2, k_3, k_4 \geq 0$ are material and temperature dependent constants. A vector field $v \in \mathcal{A}(u_{\mathrm{D}})$ locally represents the mean direction of the

*Supported by Deutsche Forschungsgemeinschaft through the DFG Research Center MATHEON 'Mathematics for key technologies' in Berlin

molecules which constitute the liquid crystal and a local minimizer of I in $\mathcal{A}(u_{\mathrm{D}})$ defines a stable configuration of the liquid crystal. The pointwise constraint $|v| = 1$ models the physically motivated assumption that in the liquid crystal phase the molecules are rod-like with a fixed length.

Existence of (global) minimizers of I in $\mathcal{A}(u_{\mathrm{D}})$ can be established if $\mathcal{A}(u_{\mathrm{D}}) \neq \emptyset$ [15]. Sufficient for $\mathcal{A}(u_{\mathrm{D}}) \neq \emptyset$ is that u_{D} is Lipschitz continuous on $\partial\Omega$ [15]. Owing to the non-convex constraint $|v| = 1$ uniqueness and higher regularity of solutions cannot be expected [15, 16, 27, 28, 29, 30, 31]. Typically, stable points of I in $\mathcal{A}(u_{\mathrm{D}})$ are not continuous and have point singularities which correspond to defects in the nematic material. In addition to non-uniqueness and existence of singularities, the non-convex nature of the problem makes it extremely difficult to numerically approximate stationary points. The crux in the design of numerical schemes lies in a stable realization of the constraint $|v| = 1$. In order to make the main ideas for the approximation of the constraint more clear we will only investigate the physically relevant one-constant approximation of I, which assumes $k_1 = k_2 = k_3 = 1$ and $k_4 = 0$ and reduces the minimization problem to the problem of finding harmonic maps:

$$(\mathrm{P}) \qquad \begin{cases} \textit{Find } u \in \mathcal{A}(u_{\mathrm{D}}) \textit{ which is a local minimizer for} \\ E : \mathcal{A}(u_{\mathrm{D}}) \to \mathbb{R},\ v \mapsto \dfrac{1}{2}\displaystyle\int_\Omega |Dv|^2 \,\mathrm{d}x. \end{cases}$$

Solutions of (P) will be called *harmonic maps*. They satisfy the Euler-Lagrange equations

$$-\Delta u = |Du|^2 u, \quad |u| = 1 \qquad \text{in } \Omega.$$

Iterative algorithms for the approximation of harmonic maps have been proposed in [10, 21, 9] and successfully been tested numerically. Convergence of an iterative scheme on a continuous level and stability of a related finite difference discretization have been proved in [1]. The goal of this work is to analyze finite element discretizations of that algorithm which allow for local mesh refinement and thereby a more efficient resolution of point singularities of solutions. We prove that, in general, finite element discretizations cannot be expected to be stable and are convergent only on structured triangulations. Sufficient for stability and convergence is that the the underlying triangulation is of acute type (cf. Lemma 3.2 for details). We provide an a posteriori criterion that allows to monitor reliability of the algorithm on general triangulations and gives rise to automatic local mesh refinement. Numerical experiments indicate that adaptive strategies are more efficient when compared to schemes on uniform triangulations. While we restrict the analysis to the one-constant approximation of I we stress that the ideas can be carried over to the full model and refer the reader to [2] for related ideas.

An alternative approach to approximating local minimizers of I consists in regularizing the problem by introducing a penalty term $\varepsilon^{-2}\big\||v|^2 - 1\big\|^2_{L^2(\Omega)}$ in I with $0 < \varepsilon \ll 1$ in order to approximate the constraint $|v| = 1$. Difficulties in analyzing such an approach stem from the lack of regularity of minimizers of I and a reliable discretization of the gradient flow of the penalized formulation generally requires very small time step sizes which limit the practical use. For related approaches and the numerical analysis of more sophisticated models we refer the reader to [3, 4, 22, 23, 25, 13].

The rest of this article is organized as follows. We briefly recall the definition and the main properties of the iterative algorithm of [1] in Section 2. Section 3 discusses finite element discretizations of that algorithm and gives sufficient a priori conditions for its convergence. A few numerical experiments show the efficiency of the discrete algorithm and are presented in Section 4. Section 5 is devoted to an a posteriori analysis and introduces local refinement indicators. The efficient performance of the resulting adaptive strategy is illustrated by some numerical experiments in Section 6.

2. ALOUGES' ALGORITHM

For an initial $u^{(0)} \in \mathcal{A}(u_{\rm D})$ Alouges' algorithm computes a sequence $\big(u^{(j)} : j \in \mathbb{N}\big) \subseteq H^1(\Omega;\mathbb{R}^3)$ by iterating the following two steps:

(A_1) Let $w^{(j)} \in K_{u^{(j)}}$ satisfy $\quad E(u^{(j)} - w^{(j)}) \le E(u^{(j)} - v) \quad$ for all $v \in K_{u^{(j)}}$, where $K_{u^{(j)}} := \{v \in H^1(\Omega;\mathbb{R}^3) :\, v|_{\partial\Omega} = 0,\, v \cdot u^{(j)} = 0 \text{ a.e. in } \Omega\}$.

(A_2) Set $u^{(j+1)} := \dfrac{u^{(j)} - w^{(j)}}{|u^{(j)} - w^{(j)}|}$.

Given any $u^{(j)} \in H^1(\Omega;\mathbb{R}^3)$ step (A_1) consists in minimizing an elliptic functional on a subspace of $H^1(\Omega;\mathbb{R}^3)$ and admits a unique solution $w^{(j)} \in K_{u^{(j)}}$. Supposing that $|u^{(j)}| = 1$ almost everywhere in Ω, the definition of $K_{u^{(j)}}$ yields

$$|u^{(j)} - w^{(j)}|^2 = |u^{(j)}|^2 + |w^{(j)}|^2 \ge 1$$

almost everywhere in Ω. Hence, $u^{(j+1)}$ in step (A_2) is well defined and satisfies $|u^{(j+1)}| = 1$ almost everywhere in Ω. It is not difficult to verify that for a function $v \in H^1(\Omega;\mathbb{R}^3)$ satisfying $|v| \ge 1$ almost everywhere in Ω there holds

$$E\Big(\frac{v}{|v|}\Big) \le E(v), \tag{2.1}$$

in particular $v/|v| \in H^1(\Omega;\mathbb{R}^3)$ and thus $u^{(j+1)} \in \mathcal{A}(u_{\rm D})$. Noting that $v \equiv 0 \in K_{u^{(j)}}$ it thus follows that

$$E(u^{(j+1)}) = E\Big(\frac{u^{(j)} - w^{(j)}}{|u^{(j)} - w^{(j)}|}\Big) \le E(u^{(j)} - w^{(j)}) \le E(u^{(j)}).$$

This is the energy decreasing property of Alouges' algorithm. The main features of the iteration are summarized in the following theorem.

Theorem 2.1 ([1])**.** *Let $u^{(0)} \in \mathcal{A}(u_{\rm D})$. Suppose that the sequences $\big(u^{(j)} : j \in \mathbb{N}\big)$ and $\big(w^{(j)} : j \in \mathbb{N}\big)$ are generated by iterating (A_1) and (A_2). Then, for all $j \in \mathbb{N}$ there holds*

$$u^{(j)} \in \mathcal{A}(u_{\rm D}) \quad \textit{and} \quad E(u^{(j+1)}) \le E(u^{(j)}).$$

There holds $w^{(j)} \to 0$ (strongly) in H^1 and there exists a subsequence $(u^{(k)} : k \in \mathbb{N})$ and a harmonic map $u^* \in \mathcal{A}(u_{\rm D})$ such that $u^{(k)} \rightharpoonup u^*$ (weakly) in H^1.

3. FE DISCRETIZATION AND NUMERICAL ANALYSIS OF (A_1) AND (A_2)

In order to make difficulties in a finite element discretization of (A_1) and (A_2) more clear we will occasionally consider a two-dimensional situation in this section. Therefore, we assume that $n = 2$ or $n = 3$ and that Ω is a bounded, polygonal or polyhedral respectively, Lipschitz domain in $\mathbb{R}^n$. Given a regular triangulation $\mathcal{T}$ of Ω into triangles ($n = 2$) or tetrahedra ($n = 3$), let $\mathcal{N}$ denote the set of nodes in $\mathcal{T}$. The lowest order finite element space related to $\mathcal{T}$ is denoted by $\mathcal{S}^1(\mathcal{T}) \subseteq H^1(\Omega)$. The nodal basis functions $(\varphi_z : z \in \mathcal{N}) \subseteq \mathcal{S}^1(\mathcal{T})$ satisfy $\varphi_z(z) = 1$ and $\varphi_z(z') = 0$ for $z \in \mathcal{N}$ and $z' \in \mathcal{N} \setminus \{z\}$. We define $\mathcal{S}^1_0(\mathcal{T}) := \{v_h \in \mathcal{S}^1(\mathcal{T}) : v_h|_{\partial\Omega} = 0\}$. Throughout this section, m is a positive integer.

The pointwise constraint $|v_h| = 1$ is satisfied solely by functions $v_h \in \mathcal{S}^1(\mathcal{T})^m$ which are constant in Ω. Therefore, assuming $u_\mathrm{D} \in C(\partial\Omega; \mathbb{R}^m)$, a reasonable finite element discretization of (P) replaces $\mathcal{A}(u_\mathrm{D})$ by the set

$$\mathcal{A}_h(\mathcal{T}, u_\mathrm{D}) := \{v_h \in \mathcal{S}^1(\mathcal{T})^m : \forall z \in \mathcal{N} \cap \partial\Omega \, v_h(z) = u_\mathrm{D}(z), \forall z \in \mathcal{N} \, |v_h(z)| = 1\}$$

and seeks a local minimizer of E in $\mathcal{A}_h(\mathcal{T}, u_\mathrm{D})$:

$$(\mathrm{P}_h) \qquad \begin{cases} \textit{Find } u_h \in \mathcal{A}_h(\mathcal{T}, u_\mathrm{D}) \textit{ which is a local} \\ \textit{minimizer for } E \textit{ in } \mathcal{A}_h(\mathcal{T}, u_\mathrm{D}). \end{cases}$$

Existence of solutions for the finite dimensional problem (P_h) follow from compactness arguments. The computation of a solution however is not obvious. We propose a discrete version of Alouges' algorithm and state sufficient conditions for its stability and convergence.

Algorithm (A_h)**.** Input: $(\mathcal{T}, u_h^{(0)}, \delta)$, where $\mathcal{T}$ is a regular triangulation of Ω, $u_h^{(0)} \in \mathcal{A}_h(\mathcal{T}, u_\mathrm{D})$ is a starting value, and $\delta > 0$ is a termination parameter.

(a) Set $j := 0$.

(b) Solve the optimization problem

$$\begin{cases} \text{Minimize} & E(u_h^{(j)} - v_h) \\ \text{subject to} & v_h \in \mathcal{S}^1_0(\mathcal{T})^m \text{ and } v_h(z) \cdot u_h^{(j)}(z) = 0 \text{ for all } z \in \mathcal{N}. \end{cases}$$

Denote the solution by $w_h^{(j)}$.

(c) If $||Dw_h^{(j)}||_{L^2(\Omega)} \leq \delta$ set $(u_h, w_h) := (u_h^{(j)}, w_h^{(j)})$ and stop.

(d) Define

$$u_h^{(j+1)} := \sum_{z \in \mathcal{N}} \frac{u_h^{(j)}(z) - w_h^{(j)}(z)}{|u_h^{(j)}(z) - w_h^{(j)}(z)|} \varphi_z.$$

(e) Set $j := j + 1$ and go to (b).

Output: $(u_h, w_h) \in \mathcal{A}_h(\mathcal{T}, u_\mathrm{D}) \times \mathcal{S}^1_0(\mathcal{T})^m$.

A discrete version of (2.1) is necessary for stability of step (d) in the algorithm. It will turn out that such an estimate in general only holds on acute type triangulations.

3.1. **Validity and possible failure of an energy decreasing property of** (A_h)**.** The following definition gives a sufficient criterion for stability of step (d) in Algorithm (A_h).

Definition 3.1. *A regular triangulation $\mathcal{T}$ of Ω is said to satisfy* an energy decreasing condition (ED) *if for all $v_h \in \mathcal{S}^1(\mathcal{T})^m$ satisfying $|v_h(z)| \geq 1$ for all $z \in \mathcal{N}$, $|v_h(z)| = 1$ for all $z \in \mathcal{N} \cap \partial\Omega$, and $w_h \in \mathcal{S}^1(\mathcal{T})^m$ defined by*

$$w_h := \sum_{z \in \mathcal{N}} \frac{v_h(z)}{|v_h(z)|} \varphi_z$$

there holds

$$E(w_h) \leq E(v_h).$$

The next lemma implies that acute type triangulations [18] allow for condition (ED).

Lemma 3.2. *Let $\mathcal{T}$ be a regular triangulation of Ω and suppose that $\int_\Omega \nabla\varphi_z \cdot \nabla\varphi_y \,\mathrm{d}x \leq 0$ for all $z \in \mathcal{N} \setminus \partial\Omega$ and $y \in \mathcal{N} \setminus \{z\}$. Then $\mathcal{T}$ satisfies condition* (ED).

Proof. For $z, y \in \mathcal{N}$ set $k_{zy} := \int_\Omega \nabla\varphi_z \cdot \nabla\varphi_y \,\mathrm{d}x$. Let $\phi_h \in \mathcal{S}^1(\mathcal{T})^m$ and define $\phi_z := \phi_h(z)$ for all $z \in \mathcal{N}$. Since $\sum_{y \in \mathcal{N}} k_{zy} = 0$ for all $z \in \mathcal{N}$ and since $k_{zy} = k_{yz}$ for all $z, y \in \mathcal{N}$ we have

$$\begin{aligned} ||\nabla\phi_h||^2_{L^2(\Omega)} &= \sum_{z,y \in \mathcal{N}} k_{zy} \phi_z \cdot \phi_y = \sum_{z,y \in \mathcal{N}} k_{zy} \phi_z \cdot (\phi_y - \phi_z) \\ &= \frac{1}{2} \sum_{z,y \in \mathcal{N}} k_{zy} \phi_z \cdot (\phi_y - \phi_z) + \frac{1}{2} \sum_{z,y \in \mathcal{N}} k_{zy} \phi_y \cdot (\phi_z - \phi_y) = -\frac{1}{2} \sum_{z,y \in \mathcal{N}} k_{zy} |\phi_z - \phi_y|^2. \end{aligned}$$

Suppose that v_h and w_h are as in Definition 3.1 and let $v_z := v_h(z)$ and $w_z := w_h(z)$ for $z \in \mathcal{N}$. Let $z, y \in \mathcal{N}$ be such that $z \neq y$. If $z \in \mathcal{N} \setminus \partial\Omega$ or $y \in \mathcal{N} \setminus \partial\Omega$ we have $k_{zy} \leq 0$ and hence by Lipschitz-continuity of the mapping $\{s \in \mathbb{R}^m : |s| \geq 1\} \to \mathbb{R}^m$, $s \mapsto s/|s|$, with Lipschitz constant 1 that

$$-\frac{1}{2} k_{zy} |w_z - w_y|^2 = -\frac{1}{2} k_{zy} \Big| \frac{w_z}{|w_z|} - \frac{w_y}{|w_y|} \Big|^2 \leq -\frac{1}{2} k_{zy} |v_z - v_y|^2.$$

If $z, y \in \mathcal{N} \cap \partial\Omega$ we have $w_z = v_z$ and $w_y = v_y$ and hence

$$||\nabla w_h||^2_{L^2(\Omega)} = -\frac{1}{2} \sum_{z,y \in \mathcal{N}} k_{zy} |w_z - w_y|^2 \leq -\frac{1}{2} \sum_{z,y \in \mathcal{N}} k_{zy} |v_z - v_y|^2 = ||\nabla v_h||^2_{L^2(\Omega)},$$

which proves the lemma. □

Remark 3.3. *(i) Suppose $n = 2$. Given neighboring nodes $z \in \mathcal{N} \setminus \partial\Omega$ and $y \in \mathcal{N} \setminus \{z\}$ let $T_1, T_2 \in \mathcal{T}$ be such that $T_1 \cap T_2$ equals the interior edge connecting z and y. Let $\alpha^{(1)}_{zy}$ and $\alpha^{(2)}_{zy}$ be the angles of T_1 and T_2, respectively, opposite to the edge connecting z and y. There holds* [11]

$$\int_\Omega \nabla\varphi_z \cdot \nabla\varphi_y \,\mathrm{d}x = -\cot\alpha^{(1)}_{zy} - \cot\alpha^{(2)}_{zy}.$$

Sufficient for $\int_\Omega \nabla\varphi_z \cdot \nabla\varphi_y \,\mathrm{d}x \leq 0$ is that $\alpha^{(1)}_{zy} + \alpha^{(2)}_{zy} \leq \pi$.
(ii) Suppose $n = 3$ and let $z \in \mathcal{N} \setminus \partial\Omega$ and $y \in \mathcal{N} \setminus \{z\}$ be such that $z, y \in T$ for some

$T \in \mathcal{T}$. Given any $T \in \mathcal{T}$ such that $z, y \in \mathcal{N} \cap T$ let α_{zyT} be the angle between the two faces $F_{zyT}^{(1)}, F_{zyT}^{(2)} \subseteq \partial T$ which do not contain both z and y. There holds [18]

$$\int_\Omega \nabla\varphi_z \cdot \nabla\varphi_y \,\mathrm{d}x = -\sum_{T\in\mathcal{T},\, z,y\in\mathcal{N}\cap T} \frac{|F_{zyT}^{(1)}|\,|F_{zyT}^{(2)}|}{9|T|} \cos\alpha_{zyT},$$

where $|F_{zyT}^{(\ell)}|$ is the surface measure of $F_{zyT}^{(\ell)}$ for $\ell = 1, 2$ and $|T|$ denotes the volume of T. Sufficient for $\int_\Omega \nabla\varphi_z \cdot \nabla\varphi_y \,\mathrm{d}x \le 0$ is that $\alpha_{zyT} \le \pi/2$ for all $T \in \mathcal{T}$ such that $z, y \in \mathcal{N} \cap T$.

The conditions of Remark 3.3 are sharp in the sense of the following example.

Example 3.4. *Let $0 < \beta < 1/2$ and $\Omega := (0,1) \times (0,\beta)$. Let*

$$\begin{aligned} &z_1 := (0,0), && z_2 := (1/2,0), && z_3 := (1,0), && z_4 := (0,\beta),\\ &z_5 := (1/2,\beta), && z_6 := (1,\beta), && z_7 := (1/4,\beta/2), && z_8 := (3/4,\beta/2) \end{aligned}$$

and $\mathcal{T} := \{T_1, T_2, ..., T_8\}$ be defined through

$$\begin{aligned} &T_1 := \mathrm{conv}\{z_1, z_2, z_7\}, && T_2 := \mathrm{conv}\{z_2, z_8, z_7\}, && T_3 := \mathrm{conv}\{z_2, z_3, z_8\},\\ &T_4 := \mathrm{conv}\{z_3, z_6, z_8\}, && T_5 := \mathrm{conv}\{z_8, z_6, z_5\}, && T_6 := \mathrm{conv}\{z_7, z_8, z_5\},\\ &T_7 := \mathrm{conv}\{z_7, z_5, z_4\}, && T_8 := \mathrm{conv}\{z_1, z_7, z_4\}, \end{aligned}$$

cf. Figure 1. Define $s := 1/2 - \beta$ and set $v_j := (1,0)$ for $j = 1, 2, ..., 6$, $v_7 := (-1,0)$, and $v_8 := (1,-s)$. Let $v_h, w_h \in \mathcal{S}^1(\mathcal{T})^2$ be such that $v_h(z_j) = v_j$ and $w_h(z_j) = w_j := v_j/|v_j|$ for $j = 1, 2, ..., 8$. There holds

$$E(w_h) > E(v_h).$$

Proof. For $j, \ell = 1, 2, ..., 8$ set $k_{j\ell} := \int_\Omega \nabla\varphi_{z_j} \cdot \nabla\varphi_{z_\ell} \,\mathrm{d}x$. Since $w_j = v_j$ for $j = 1, 2, ..., 7$ we have (cf. the proof of Lemma 3.2)

$$\delta := ||\nabla v_h||_{L^2(\Omega)}^2 - ||\nabla w_h||_{L^2(\Omega)}^2 = -\frac{1}{2}\sum_{j,\ell=1}^{8} k_{j\ell}\big(|v_j - v_\ell|^2 - |w_j - w_\ell|^2\big)$$

$$= -\sum_{j=1}^{6} k_{j8}\big(|(1,0) - v_8|^2 - |(1,0) - w_8|^2\big) - k_{78}\big(|(-1,0) - v_8|^2 - |(-1,0) - w_8|^2\big).$$

We use $|(1,0) - v_8|^2 = s^2$, $|(-1,0) - v_8|^2 = 4 + s^2$ and abbreviate

$$\kappa_1^2 := |(1,0) - w_8|^2 = 2 - 2/\sqrt{1+s^2}, \quad \kappa_2^2 := |(-1,0) - w_8|^2 = 2 + 2/\sqrt{1+s^2}.$$

Using that $\sum_{j=1}^{8} k_{j8} = 0$ we verify $\sum_{j=1}^{6} k_{j8} = -k_{78} - k_{88}$ and obtain

$$\delta = (s^2 - \kappa_1^2)(k_{78} + k_{88}) - k_{78}(4 + s^2 - \kappa_2^2) = k_{88}(s^2 - \kappa_1^2) - k_{78}(4 + \kappa_1^2 - \kappa_2^2).$$

Elementary calculations show that

$$k_{88} = (12\beta^2 + 5)/(4\beta), \qquad k_{78} = (1 - 4\beta^2)/(4\beta).$$

With a function ϕ such that $\sqrt{1+s^2} = 1 + \frac{1}{2}s^2 + \phi(s^2)$ we deduce

$$4\beta\sqrt{1+s^2}\delta = \big(12\beta^2+5\big)\big(\frac{1}{2}s^4 + s^2\phi(s^2) - 2\phi(s^2)\big) - \big(1-4\beta^2\big)\big(2s^2+4\phi(s^2)\big).$$

Using that $\beta^2 = \frac{1}{4} - s + s^2$ we verify

$$\begin{aligned} 4\beta\sqrt{1+s^2}\delta &= \big(8-12s+12s^2\big)\big(\frac{1}{2}s^4 + s^2\phi(s^2) - 2\phi(s^2)\big) - 16\big(s-s^2\big)\big(\frac{1}{2}s^2 + \phi(s^2)\big) \\ &= -8s^3 + 12s^4 - 6s^5 + 6s^6 + \phi(s^2)\big(-16 + 8s - 12s^3 + 12s^4\big) \\ &= -6s^3\big(1-2s\big) - 6s^5(1-s) + 4s\phi(s^2)\big(2-3s^2+3s^3\big) - 2\big(s^3 + 8\phi(s^2)\big). \end{aligned}$$

Since $0 < s < 1/2$ and $\phi(s^2) < 0$, the first three terms on the right-hand side are negative. A Taylor expansion proves $-s^4/8 \le \phi(s^2)$ and implies that the last term on the right-hand side is non-positive. This shows $\delta < 0$ and proves the lemma. $\square$

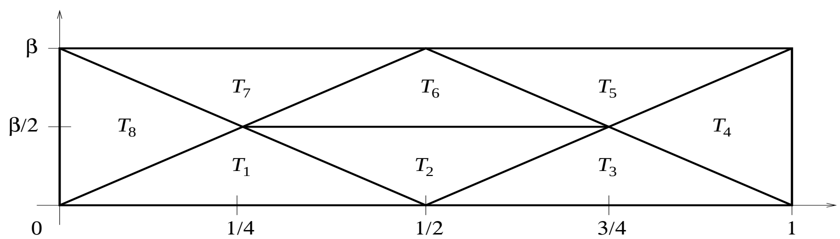

FIGURE 1. Triangulation $\mathcal{T}$ in Example 3.4 that does not satisfy condition (ED) for $0 < \beta < 1/2$.

We include another sufficient criterion for validity of condition (ED) that allows to construct triangulations of a large class of three-dimensional domains.

Lemma 3.5. *Suppose $n = 3$ and assume that each $T \in \mathcal{T}$ has three mutually perpendicular edges. Then $\mathcal{T}$ satisfies condition* (ED).

Proof. Let $v_h, w_h \in \mathcal{S}^1(\mathcal{T})^m$ be as in Definition 3.1 and let $T \in \mathcal{T}$. Let $b_1, b_2, b_3 \in \mathbb{R}^3 \setminus \{0\}$ be mutually perpendicular and such that $b_j = z_j - y_j$, $j = 1,2,3$, where $z_j, y_j \in \mathcal{N} \cap T$ for $j = 1,2,3$. After an appropriate rotation we may assume $b_j = |b_j|e_j$ for $j = 1,2,3$, where e_j is the j-th canonical basis vector in $\mathbb{R}^3$. Since $s \mapsto s/|s|$ for $s \in \mathbb{R}^m$ with $|s| \ge 1$ is Lipschitz continuous with Lipschitz constant 1 we deduce for $j = 1,2,3$ that

$$\Big|\frac{\partial w_h|_T}{\partial x_j}\Big| = \frac{1}{|z_j - y_j|}\Big|\frac{v_h(z_j)}{|v_h(z_j)|} - \frac{v_h(y_j)}{|v_h(y_j)|}\Big| \le \frac{1}{|z_j - y_j|}|v_h(z_j) - v_h(y_j)| = \Big|\frac{\partial v_h|_T}{\partial x_j}\Big|,$$

which implies the lemma. $\square$

Remark 3.6. *It can be shown* [17] *that if $n = 3$ and each $T \in \mathcal{T}$ has 3 mutually perpendicular edges which do not pass through the same vertex then $\mathcal{T}$ is of acute type, i.e., satisfies the conditions of Remark 3.3 (ii).*

The following example defines a triangulation of the unit cube which satisfies the conditions of Lemma 3.5. It allows to construct triangulations that satisfy condition (ED) of unions of finitely many quadrilaterals. Other constructions and acute type refinement strategies of tetrahedra can be found in [18, 17].

Example 3.7 ([19, 5])**.** *Set* $\mathcal{N} := \{z_1, z_2, ..., z_8\}$ *for*

$$z_1 := (0,0,0), \quad z_2 := (1,0,0), \quad z_3 := (0,0,1), \quad z_4 := (1,0,1),$$
$$z_5 := (0,1,0), \quad z_6 := (1,1,0), \quad z_7 := (0,1,1), \quad z_8 := (1,1,1).$$

Define $\mathcal{T} := \{T_1, T_2, ..., T_6\}$ *with*

$$T_1 := \mathrm{conv}\{z_1, z_2, z_3, z_6\}, \quad T_2 := \mathrm{conv}\{z_2, z_4, z_3, z_6\}, \quad T_3 := \mathrm{conv}\{z_3, z_4, z_8, z_6\},$$
$$T_4 := \mathrm{conv}\{z_3, z_8, z_7, z_6\}, \quad T_5 := \mathrm{conv}\{z_7, z_5, z_3, z_6\}, \quad T_6 := \mathrm{conv}\{z_3, z_5, z_1, z_6\}.$$

Then $\mathcal{T}$ *is a regular triangulation of* $(0,1)^3$ *and satisfies the assumptions of Lemma 3.5, cf. Figure 2.* □

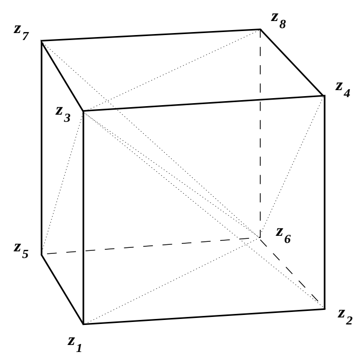

FIGURE 2. Triangulation $\mathcal{T}$ of the unit cube defined in Example 3.7 such that each element in $\mathcal{T}$ has three mutually perpendicular edges.

3.2. **Well-posedness and termination of Algorithm** (A_h)**.** The following lemma shows that all steps in (A_h) are well defined and that the algorithm terminates within a finite number of iterations, provided that $\mathcal{T}$ satisfies condition (ED).

Lemma 3.8. *Suppose* $\mathcal{T}$ *satisfies condition* (ED)*. Given* $\delta > 0$ *and* $u_h^{(0)} \in \mathcal{A}_h(\mathcal{T}, u_\mathrm{D})$*, Algorithm* (A_h) *with input* $(\mathcal{T}, u_h^{(0)}, \delta)$ *terminates within a finite number* M *of iterations with output* $(u_h, w_h) \in \mathcal{A}_h(\mathcal{T}, u_\mathrm{D}) \times \mathcal{S}_0^1(\mathcal{T})^m$ *such that* $||Dw_h||_{L^2(\Omega)} \le \delta$ *and*

$$E(u_h) \le E(u_h^{(0)}).$$

Proof. We proceed by induction to show $u_h^{(j)} \in \mathcal{A}_h(\mathcal{T}, u_\mathrm{D})$ and $E(u_h^{(j+1)}) \le E(u_h^{(j)})$. Suppose that for some $j \ge 0$ we are given $u_h^{(j)} \in \mathcal{A}_h(\mathcal{T}, u_\mathrm{D})$. The set

$$L^{(j)} := \left\{v_h \in \mathcal{S}_0^1(\mathcal{T})^m : \forall z \in \mathcal{N}\ v_h(z) \cdot u_h^{(j)}(z) = 0\right\}$$

is a subspace of $\mathcal{S}_0^1(\mathcal{T})^m$. Hence, there exists $w_h \in L^{(j)}$ such that

$$\int_\Omega Dw_h : Dv_h \,\mathrm{d}x = \int_\Omega Du_h^{(j)} : Dv_h \,\mathrm{d}x \tag{3.1}$$

for all $v_h \in L^{(j)}$. This is equivalent to

$$E(u_h^{(j)} - w_h) \leq E(u_h^{(j)} - v_h)$$

for all $v_h \in L^{(j)}$. Thus, $w_h = w_h^{(j)}$ is the unique solution in step (b) of Algorithm (A_h). Since $w_h^{(j)}(z) \cdot u_h^{(j)}(z) = 0$ and $|u_h^{(j)}(z)| = 1$ there holds $|u_h^{(j)}(z) - w_h^{(j)}(z)| \geq 1$ for all $z \in \mathcal{N}$. Hence, $u_h^{(j+1)}$ is well defined and $u_h^{(j+1)} \in \mathcal{A}_h(\mathcal{T}, u_\mathrm{D})$. Since $0 \in L^{(j)}$ and $\mathcal{T}$ satisfies condition (ED) there holds $E(u_h^{(j+1)}) \leq E(u_h^{(j)} - w_h^{(j)}) \leq E(u_h^{(j)})$. Equation (3.1) with $v_h = w_h = w_h^{(j)}$ proves $E(u_h^{(j)} - w_h^{(j)}) = E(u_h^{(j)}) - E(w_h^{(j)})$ and a combination with the previous assertion shows

$$0 \leq E(w_h^{(j)}) \leq E(u_h^{(j)}) - E(u_h^{(j+1)}).$$

Since $\big(E(u_h^{(j)}) : j \in \mathbb{N}\big)$ is monotonically decreasing and bounded from below we conclude that it is a Cauchy sequence and hence $||Dw_h^{(M)}||_{L^2(\Omega)} \leq \delta$ for M sufficiently large. □

3.3. **Convergence for $h \to 0$.** The following theorem shows that for a sequence of triangulations with maximal mesh-size tending to 0 the sequence of outputs of Algorithm (A_h) provides a weakly convergent subsequence whose weak limit is a harmonic map. The important questions whether this weak limit is (globally) energy minimizing in (P) or whether weak convergence can be improved to strong convergence are left for future research.

Theorem 3.9. *Suppose $u_\mathrm{D} \in H^1(\partial\Omega; \mathbb{R}^3)$. Let $(\mathcal{T}_k : k \in \mathbb{N})$ be a sequence of regular triangulations of Ω satisfying condition (ED) with maximal mesh-sizes $(h_k : k \in \mathbb{N})$ satisfying $h_k \to 0$ for $k \to \infty$ and let $(\delta_k : k \in \mathbb{N})$ be a sequence of positive numbers such that $\delta_k \to 0$ for $k \to \infty$. Suppose that $u_k^{(0)} \in \mathcal{A}_h(\mathcal{T}_k, u_\mathrm{D})$ and there exists $C_0 > 0$ such that*

$$||Du_k^{(0)}||_{L^2(\Omega)} \leq C_0$$

for all $k \in \mathbb{N}$. For each $k \in \mathbb{N}$, let (u_k, w_k) be the output of Algorithm (A_h) applied to the input $(\mathcal{T}_k, u_k^{(0)}, \delta_k)$. Then there exists a subsequence $(u_\ell : \ell \in \mathbb{N})$ and a harmonic map $u^* \in \mathcal{A}(u_\mathrm{D})$ such that $u_\ell \rightharpoonup u^*$ (weakly) in H^1 and

$$E(u^*) \leq \liminf_{\ell \to \infty} E(u_\ell).$$

The following lemma is essential in the proof of the theorem. For $c \in \mathbb{R}^3$ and a matrix $A \in \mathbb{R}^{3\times 3}$ with columns $a_1, a_2, a_3 \in \mathbb{R}^3$ we let $c \times A \in \mathbb{R}^{3\times 3}$ be the matrix whose columns equal $c \times a_j$ for $j = 1, 2, 3$.

Lemma 3.10 ([8])**.** *A function $u \in \mathcal{A}(u_\mathrm{D})$ is a harmonic map if and only if*

$$\int_\Omega \big(u \times Du\big) : D\phi \,\mathrm{d}x = 0 \tag{3.2}$$

for all $\phi \in H_0^1(\Omega; \mathbb{R}^3) \cap L^\infty(\Omega; \mathbb{R}^3)$.

Proof. Suppose that u is a harmonic map, i.e., for all $w \in H^1_0(\Omega;\mathbb{R}^3) \cap L^\infty(\Omega;\mathbb{R}^3)$ there holds

$$\int_\Omega Du : Dw \,\mathrm{d}x = \int_\Omega |Du|^2 u \cdot w \,\mathrm{d}x.$$

Let $\phi \in H^1_0(\Omega;\mathbb{R}^3) \cap L^\infty(\Omega;\mathbb{R}^3)$ and set $w := u \times \phi$. Using $(a \times b) \cdot c = -(a \times c) \cdot b$ for any $a, b, c \in \mathbb{R}^3$ we verify

$$Du : Dw = Du : \big(Du \times \phi + u \times D\phi\big) = Du : \big(u \times D\phi\big) = -\big(u \times Du\big) : D\phi$$

almost everywhere in Ω and since $u \cdot w = 0$ we find that u satisfies (3.2). Suppose now that u satisfies (3.2) and set $\phi := u \times w$. The identity $(a \times b) \cdot (c \times d) = (a \cdot c)(b \cdot d) - (b \cdot c)(a \cdot d)$ yields

$$\begin{aligned} D(u \times w) : \big(u \times Du\big) &= \big(Du \times w\big) : \big(u \times Du\big) + \big(u \times Dw\big) : \big(u \times Du\big) \\ &= \big(u^T Du\big) \cdot \big(w^T Du\big) - |Du|^2 u \cdot w + |u|^2 Dw : Du - \big(u^T Dw\big) \cdot \big(u^T Du\big) \end{aligned}$$

almost everywhere in Ω. The identity $|u|^2 = 1$ implies $u^T Du = 0$ almost everywhere in Ω. An integration over Ω finishes the proof of the lemma. □

Proof of Theorem 3.9. By Lemma 3.8 and the boundedness of $(u_k^{(0)})$ in H^1 there holds $||Du_k||_{L^2(\Omega)} \le ||Du_k^{(0)}||_{L^2(\Omega)} \le C_0$ for all $k \in \mathbb{N}$. Hence, there exists a subsequence $(u_\ell : \ell \in \mathbb{N})$ and $u^* \in H^1(\Omega;\mathbb{R}^3)$ such that $u_\ell \rightharpoonup u^*$ (weakly) in H^1. Weak lower semi-continuity of E implies $E(u^*) \le \liminf_{\ell\to\infty} E(u_\ell)$. Since $|u_\ell(z)| = 1$ for all $z \in \mathcal{N}_\ell$ we have, by a $\mathcal{T}$ elementwise application of Poincaré's inequality and $|u_\ell| \le 1$ almost everywhere in Ω,

$$||\, |u_\ell|^2 - 1\, ||_{L^2(\Omega)} \le C_P h_\ell ||2 u_\ell^T D u_\ell||_{L^2(\Omega)} \le 2 C_P C_0 h_\ell.$$

Since $u_\ell \to u^*$ almost everywhere in Ω we deduce $|u^*| = 1$ almost everywhere in Ω. Moreover, we have

$$\big\|u_\ell|_{\partial\Omega} - u_{\mathrm{D}}\big\|_{L^2(\partial\Omega)} \le C h_\ell \big\|\partial u_{\mathrm{D}}/\partial s||_{L^2(\partial\Omega)}$$

(here, $\partial u_{\mathrm{D}}/\partial s$ denotes the surface gradient of u_{D} along $\partial\Omega$) and compactness of the trace operator as a mapping from $H^1(\Omega;\mathbb{R}^3)$ into $L^2(\partial\Omega;\mathbb{R}^3)$ (cf. [26] for details) implies $u^*|_{\partial\Omega} = u_{\mathrm{D}}$. It remains to show that u^* is a harmonic map. For all $\Psi_\ell \in \mathcal{S}^1_0(\mathcal{T}_\ell)^3$ with $\Psi_\ell(z) \cdot u_\ell(z) = 0$ for all $z \in \mathcal{N}_\ell$ there holds by definition of w_ℓ

$$\int_\Omega D(u_\ell - w_\ell) : D\Psi_\ell \,\mathrm{d}x = 0.$$

Given $\phi \in C^\infty_0(\Omega;\mathbb{R}^3)$ let $\Phi_\ell := \phi \times u_\ell$ and choose $\Psi_\ell := \mathcal{I}_\ell(\phi \times u_\ell)$, where $\mathcal{I}_\ell$ denotes the nodal interpolation operator on $\mathcal{T}_\ell$. We then have

$$\int_\Omega Du_\ell : D(\phi \times u_\ell) \,\mathrm{d}x = \int_\Omega D(u_\ell - w_\ell) : D(\Phi_\ell - \Psi_\ell) \,\mathrm{d}x + \int_\Omega Dw_\ell : D\Phi_\ell \,\mathrm{d}x. \tag{3.3}$$

Using

$$Du_\ell : D(\phi \times u_\ell) = Du_\ell : (D\phi \times u_\ell + \phi \times Du_\ell) = Du_\ell : (D\phi \times u_\ell) = D\phi : (u_\ell \times Du_\ell)$$

and $u_\ell \to u^*$ (strongly) in L^2, $Du_\ell \rightharpoonup Du^*$ (weakly) in H^1 we deduce

$$\int_\Omega Du_\ell : D(\phi \times u_\ell)\,\mathrm{d}x = \int_\Omega D\phi : (u_\ell \times Du_\ell)\,\mathrm{d}x \to \int_\Omega D\phi : (u^* \times Du^*)\,\mathrm{d}x. \tag{3.4}$$

Since u_ℓ is $\mathcal{T}$ elementwise affine there holds for each $T \in \mathcal{T}$

$$\begin{aligned} ||D(\Phi_\ell - \Psi_\ell)||_{L^2(T)} &= ||D\big(\phi \times u_\ell - \mathcal{I}_\ell(\phi \times u_\ell)\big)||_{L^2(T)} \le Ch_\ell ||D^2(\phi \times u_\ell)||_{L^2(T)} \\ &\le Ch_\ell\big(||D^2\phi||_{L^2(T)} + ||D\phi||_{L^\infty(\Omega)}||Du_\ell||_{L^2(T)}\big), \end{aligned}$$

and hence $\Phi_\ell - \Psi_\ell \to 0$ (strongly) in H^1. Notice that $u_\ell - w_\ell$ is uniformly bounded in H^1 so that

$$\int_\Omega D(u_\ell - w_\ell) : D(\Phi_\ell - \Psi_\ell)\,\mathrm{d}x \to 0. \tag{3.5}$$

Since Φ_ℓ is bounded in H^1 and $w_\ell \to 0$ (strongly) in H^1 we have

$$\int_\Omega Dw_\ell : D\Phi_\ell\,\mathrm{d}x \to 0. \tag{3.6}$$

A combination of (3.3)-(3.6) yields

$$\int_\Omega D\phi : (u^* \times Du^*)\,\mathrm{d}x = 0$$

which, according to Lemma 3.10, shows that u^* is a harmonic map. □

4. Numerical experiments I

In this section we report on some numerical experiments. We first discuss the implementation of Algorithm (A_h).

4.1. **Uzawa iteration for the efficient solution of step** (b)**.** Step (b) of Algorithm (A_h) requires the solution of a quadratic optimization problem with linear constraints. This can be solved directly, but may be inefficient. We thus propose the use of an Uzawa iteration. The optimization problem may be rewritten as a saddle point problem and the related optimality conditions read:

$$(\mathrm{SP}_h) \qquad \begin{cases} \textit{Find } w_h \in \mathcal{S}^1_0(\mathcal{T})^3 \textit{ and } \lambda \in \mathbb{R}^{\mathcal{K}} \textit{ such that, for all } v_h \in \mathcal{S}^1_0(\mathcal{T})^3, \\ \displaystyle\int_\Omega Dw_h : Dv_h\,\mathrm{d}x + \sum_{z\in\mathcal{K}} \lambda_z u_h^{(j)}(z)\cdot v_h(z) = \int_\Omega Du_h^{(j)} : Dv_h\,\mathrm{d}x, \\ w_h(z)\cdot u_h^{(j)}(z) = 0 \quad \text{for all } z \in \mathcal{K}. \end{cases}$$

Here, $\mathcal{K} := \mathcal{N} \cap \Omega$ denotes the set of free nodes in $\mathcal{N}$. The problem can be recast as:

$$(\mathrm{SP}'_h) \qquad \begin{cases} \textit{Find } x \in \mathbb{R}^{3N'} \textit{ and } \lambda \in \mathbb{R}^{N'} \textit{ such that} \\ A'x + B^T\lambda = b, \\ Bx \qquad\quad\; = 0. \end{cases}$$

In this formulation, $x \in \mathbb{R}^{3N'}$ contains the values of w_h in the free nodes and we set $N' :=$ card$(\mathcal{K})$. The constraint $u_h(z)\cdot w_h(z) = 0$, $z \in \mathcal{K}$, is realized by the matrix $B \in \mathbb{R}^{3N'\times N'}$. The positive definite matrix $A' \in \mathbb{R}^{3N'\times 3N'}$ is the restriction of A to $\mathcal{S}^1_0(\mathcal{T})^3$, where A is the stiffness matrix defined through the nodal basis in $\mathcal{S}^1(\mathcal{T})^3$. Finally, b is given by the restriction of $A\underline{u}$ to the free nodes, assuming that $\underline{u}$ contains the nodal values of $u_h^{(j)}$ in $\mathcal{N}$. The efficient iterative solution of (SP'_h) is realized by an Uzawa algorithm with conjugate directions and an LU decomposition of A' (cf., e.g., [6]).

4.2. **Numerical examples.** For the first numerical experiments we specify (P) in the following example.

Example 4.1. *Set* $\Omega := (-1/2, 1/2)^3$ *and* $u_\mathrm{D}(x) := x/|x|$, $x \in \partial\Omega$. *Then,* $u(x) = x/|x|$, $x \in \Omega$*, is the unique solution of* (P) [20].

In order to satisfy the conditions that guarantee convergence in Theorem 3.9 we construct triangulations of Ω that satisfy condition (ED) by scaling, translating, and assembling copies of the triangulation $\mathcal{T}$ from Example 3.7.

Example 4.2. *Given an integer* $k \geq 1$ *set* $h_k := 1/k$*,*

$$C_k := \big\{ h_k(\ell, m, n) : \ 0 \leq \ell, m, n \leq k-1 \big\} - (1,1,1)/2,$$

and define, with $\tilde{\mathcal{T}}$ *from Example 3.7,*

$$\mathcal{T}_k := \big\{ c + h_k T : \ c \in C_k, \ T \in \mathcal{T} \big\}.$$

Then, $\mathcal{T}_k$ *is a regular triangulation of* $\Omega = (-1/2, 1/2)^3$ *with maximal mesh-size* $\sqrt{3}/k$ *and satisfies condition* (ED).

We used four triangulations $\mathcal{T}_k$, specified through $k = 4, 8, 16, 32$ in Example 4.1, with $3N'_k = 375, 2187, 14739, 107811$ degrees of freedom (i.e., N'_k free nodes in $\mathcal{T}_k$). We set $\delta_k := 10^{-4}/\log_2(k)$, and define initial functions $u_k^{(0)} \in \mathcal{A}_h(\mathcal{T}, u_\mathrm{D})$ by

$$u_k^{(0)}(z) := \begin{cases} z/|z|, & \text{for } z \in \mathcal{N}_k \cap \partial\Omega, \\ (0,1,0), & \text{for } z \in \mathcal{N}_k \cap \Omega. \end{cases}$$

In all experiments the Uzawa iteration was stopped when the ℓ^2 norm of the residual Bx in (SP'_h) was less than 10^{-6}. In most of the experiments this stopping criterion was satisfied after at most 20 iterations.

Figure 3 displays the decay of the energy $E(u_k^{(j)})$, $j = 1, 2, ...$, in the iteration of Algorithm (A_h) with input $(\mathcal{T}_k, u_k^{(0)}, \delta_k)$ for $k = 4, 8, 16, 32$. The plot shows that the decrease in the energy is largest for the first few iterations. This yields the conjecture that the choice of the termination criteria $\delta_k = 10^{-4}/\log_2 k$ is inefficient in this example if one is only interest in an asymptotic behavior for $h \to 0$.

Figure 4 shows the projection of the vector fields $u_{32}^{(j)}(0, \cdot, \cdot)$ obtained from Algorithm (A_h) onto $\{(x, y, z) \in \mathbb{R}^3 : x = 0\}$ in $(-1/2, 1/2)^2$ for $j = 0, 10, 50, 315$. We observe that only a few iterations are needed to rotate vectors in such a way that only one degree one singularity is present. The subsequent iterations move this singularity to the origin. After 317 iterations Algorithm (A_h) with input $(\mathcal{T}_{32}, u_{32}^{(0)}, \delta_{32})$ terminates and the nodal values of the output u_{32} appear to be very close to the exact solution away from 0. The value of the numerical solution at 0, where the exact solution has a singularity, has no particular meaning and seems to depend on the triangulation and the initial value.

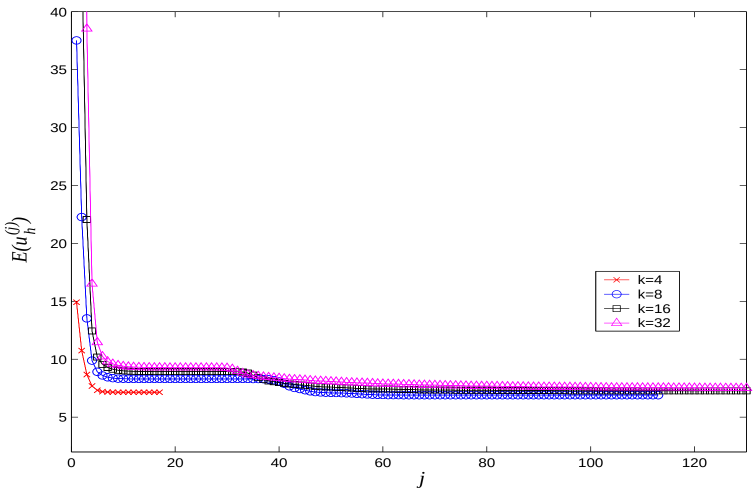

FIGURE 3. Decay of the energy in the iteration of Algorithm (A_h) on $\mathcal{T}_k$ with $k = 4, 8, 16, 32$ in Example 4.1 and initial $u_k^{(0)} \in \mathcal{A}_h(\mathcal{T}, u_{\mathrm{D}})$.

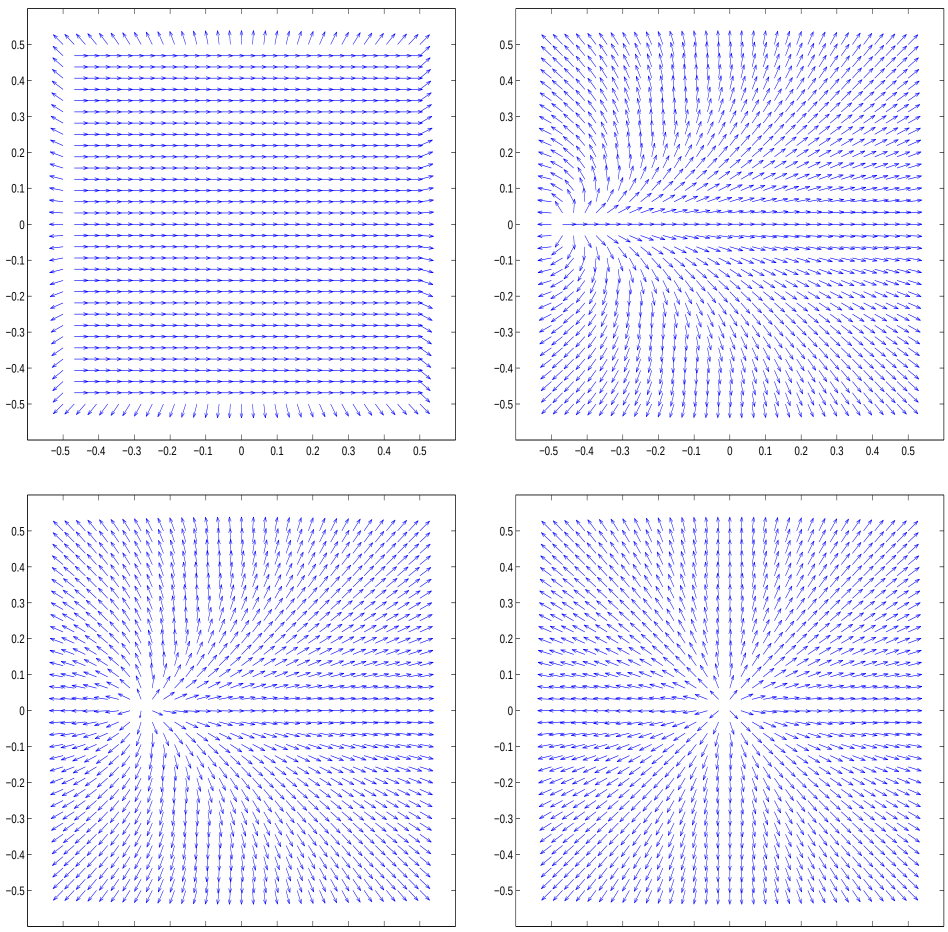

FIGURE 4. Projection of the vector fields $u_{32}^{(j)}(0, \cdot, \cdot)$ onto $\{(x, y, z) \in \mathbb{R}^3 : x = 0\}$ in $(-1/2, 1/2)^2$ for $j = 0, 10, 50, 315$ in Example 4.1 and initial $u_k^{(0)} \in \mathcal{A}_h(\mathcal{T}, u_{\mathrm{D}})$.

We assume that our definition of $u_k^{(0)}$ is suboptimal as it admits large gradients in a neighborhood of $\partial\Omega$. In particular, this choice does not satisfy $||Du_k^{(0)}||_{L^2(\Omega)} \leq C_0$ for $h_k \to 0$. However, even if for all $z \in \mathcal{K}$, $\xi(z)$ is a random unit vector in $\mathbb{R}^3$ and the starting value $\tilde{u}_k^{(0)} \in \mathcal{A}_h(\mathcal{T}, u_{\mathrm{D}})$ is defined by

$$\tilde{u}_k^{(0)}(z) := \begin{cases} z/|z|, & \text{for } z \in \mathcal{N}_k \cap \partial\Omega, \\ \xi(z), & \text{for } z \in \mathcal{N}_k \cap \Omega. \end{cases}$$

then we observe in Figure 5 that the energy still decreases rapidly in the first iterations and becomes stationary almost as fast as for the previous choice. We assume that the number of iterations depends on the initial energy and can be reduced with an optimal choice of $u_k^{(0)}$. Indeed, the proof of Lemma 3.8 shows that the sequence of corrections $w_k^{(j)}$ satisfies for all $\ell \geq 0$

$$\sum_{j=0}^{\ell} ||Dw_k^{(j)}||_{L^2(\Omega)}^2 \leq ||Du_k^{(0)}||_{L^2(\Omega)}^2,$$

and assuming that $||Du_k^{(0)}||_{L^2(\Omega)} \leq C_0$ (for a k-independent constant $C_0 > 0$) then the number of iterations can be expected to grow less fast than in the presented experiments.

Figure 6 shows the projection of the vector fields $u_{32}^{(j)}(0,\cdot,\cdot)$ onto $\{(x,y,z) \in \mathbb{R}^3 : x = 0\}$ in $(-1/2, 1/2)^2$ for $j = 0, 10, 50, 165$ produced by Algorithm (A_h) with initial data $\tilde{u}_{32}^{(0)}$. We observe that the algorithm immediately changes the highly unordered initial configuration into a more stable one; after ten iterations only one degree one singularity with high symmetry can be seen. The subsequent iterations move the singularity to the origin.

5. Local refinement criteria

The main assertion of this section is a modification of the assumptions of Theorem 3.9. It replaces the assumption that the maximal mesh-size tends to 0 and that the employed triangulations are of acute type by the weaker assumption that certain computable quantities tend to 0. Moreover, the assertion is independent of a particular scheme since the computable quantities are entirely determined by an approximation u_h.

Given a regular triangulation $\mathcal{T}$ of Ω let $h_{\mathcal{T}} \in L^\infty(\Omega)$ be the $\mathcal{T}$-elementwise constant function satisfying $h_{\mathcal{T}}|_T = \mathrm{diam}(T)$ for all $T \in \mathcal{T}$. $\mathcal{F}$ denotes the set of all faces in $\mathcal{T}$ and $h_{\mathcal{F}}$ is defined on $\cup\mathcal{F}$ through $h_{\mathcal{F}}|_F := \mathrm{diam}(F)$ for all $F \in \mathcal{F}$. For a $\mathcal{T}$-elementwise smooth (e.g., $\mathcal{T}$-elementwise constant) function $\Sigma \in L^\infty(\Omega; \mathbb{R}^{3\times 3})$ we set

$$\big[\Sigma \cdot n_{\mathcal{F}}\big]|_F := \big((\Sigma|_{T_2})|_F - (\Sigma|_{T_1})|_F\big) \cdot n_F,$$

where $F \in \mathcal{F} \cap \Omega$, $T_1, T_2 \in \mathcal{T}$ such that $T_1 \cap T_2 = F$, and $n_F \in \mathbb{R}^3$ is the unit normal vector to F pointing from T_1 into T_2.

Definition 5.1. *Given any $u_h \in \mathcal{S}^1(\mathcal{T})^3$ let $w_h \in \mathcal{S}_0^1(\mathcal{T})^3$ satisfy $w_h(z) \cdot u_h(z) = 0$ for all $z \in \mathcal{N}$ and*

$$\int_\Omega Dw_h : Dv_h \,\mathrm{d}x = \int_\Omega Du_h : Dv_h \,\mathrm{d}x$$

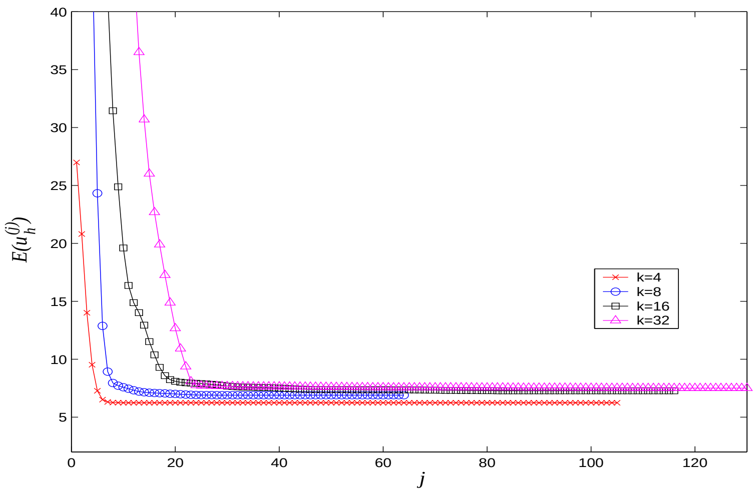

FIGURE 5. Decay of the energy in the iteration of Algorithm (A_h) on $\mathcal{T}_k$ with $k = 4, 8, 16, 32$ in Example 4.1 with random initial data $\tilde{u}_k^{(0)} \in \mathcal{A}_h(\mathcal{T}, u_{\mathrm{D}})$.

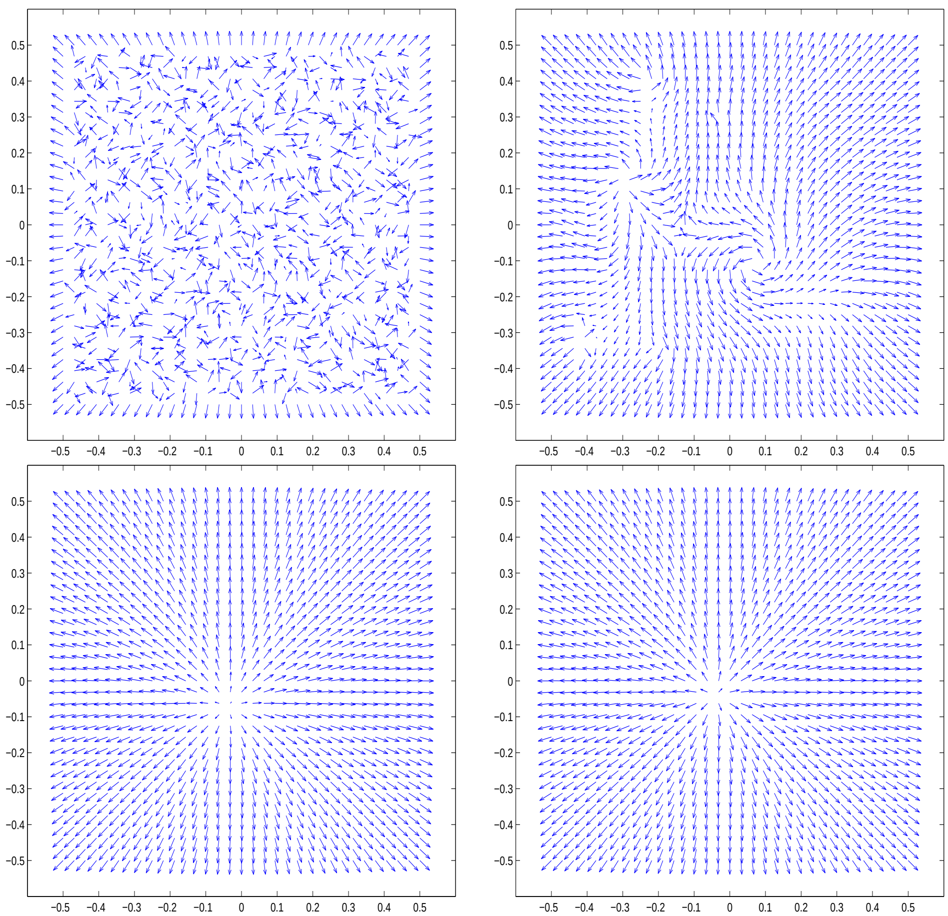

FIGURE 6. Projection of the vector fields $u_{32}^{(j)}(0,\cdot,\cdot)$ onto $\{(x,y,z) \in \mathbb{R}^3 : x = 0\}$ in $(-1/2,1/2)^2$ for $j = 0, 10, 50, 165$ in Example 4.1 with initial data $\tilde{u}_{32}^{(0)} \in \mathcal{A}_h(\mathcal{T}, u_{\mathrm{D}})$.

for all $v_h \in \mathcal{S}_0^1(\mathcal{T})^3$ *with* $v_h(z) \cdot u_h(z) = 0$ *for all* $z \in \mathcal{N}$*. For each* $T \in \mathcal{T}$ *set*

$$\eta_1(T, u_h)^2 := \big\| |u_h|^2 - 1 \big\|_{L^2(T)}^2 + \big\| u_h|_{\partial\Omega} - u_{\mathrm{D}} \big\|_{L^2(\partial T \cap \partial\Omega)}^2,$$
$$\eta_2(T, u_h)^2 := \big\| h_{\mathcal{F}}^{1/2} [D(u_h - w_h) \cdot n_{\mathcal{F}}] \big\|_{L^2(\partial T \cap \Omega)}^2 + ||Dw_h||_{L^2(T)}^2$$

Note that the following assertion does not assume that u_h is obtained by Algorithm (A_h), that the maximal mesh-sizes tend to 0, or that the triangulations satisfy condition (ED).

Proposition 5.2. *Suppose that* $(\mathcal{T}_k : k \in \mathbb{N})$ *is a sequence of regular triangulations of* Ω*, and let* $(u_k : k \in \mathbb{N}) \subseteq \mathcal{S}^1(\mathcal{T}_k)^3$ *be such that* $||Du_k||_{L^2(\Omega)} \le C_1$ *for some* $C_1 > 0$ *and all* $k \ge 0$*. Suppose that*

$$\sum_{T \in \mathcal{T}_k} \eta_1(T, u_k)^2 + \eta_2(T, u_k)^2 \to 0 \quad \textit{for } k \to \infty.$$

Then there exists a subsequence $(u_\ell : \ell \in \mathbb{N})$ *and a harmonic map* $u^* \in \mathcal{A}(u_{\mathrm{D}})$ *such that* $u_\ell \rightharpoonup u^*$ *(weakly) in* H^1 *and*

$$E(u^*) \le \liminf_{\ell \to \infty} E(u_\ell). \tag{5.1}$$

Proof. The boundedness of $||Du_k||_{L^2(\Omega)}^2 + ||u_k||_{L^2(\Omega)}^2$ implies the existence of a weakly convergent subsequence $(u_\ell : \ell \in \mathcal{N})$ and a weak limit $u^* \in H^1(\Omega; \mathbb{R}^3)$. Since $\sum_{T \in \mathcal{T}} \eta_1(T, u_\ell)^2 \to 0$ one verifies that $u^* \in \mathcal{A}(u_{\mathrm{D}})$. The weak lower semicontinuity of E proves (5.1). It remains to show that u^* is a harmonic map. Given any $\phi \in C_0^\infty(\Omega; \mathbb{R}^3)$ we set $\Phi_\ell := \phi \times u_\ell$ and let $\Psi_\ell := \mathcal{I}_\ell \Phi_\ell$ be the nodal interpolant of Φ_ℓ on $\mathcal{T}_\ell$. As in the proof of Theorem 3.9 we have to show that

$$\int_\Omega Du_\ell : D(\phi \times u_\ell)\,\mathrm{d}x = \int_\Omega D(u_\ell - w_\ell) : D(\Phi_\ell - \Psi_\ell)\,\mathrm{d}x + \int_\Omega Dw_\ell : D\Phi_\ell\,\mathrm{d}x \to 0.$$

A $\mathcal{T}_\ell$-elementwise integration by parts and standard interpolation estimates yield

$$\begin{aligned}\int_\Omega D(u_\ell - w_\ell) : D(\Phi_\ell - \Psi_\ell)\,\mathrm{d}x &= \sum_{F \in \mathcal{F}_\ell,\, F \subseteq \Omega} \int_F [D(u_h - w_h) \cdot n_{\mathcal{F}_\ell}] \cdot (\Phi_\ell - \Psi_\ell)\,\mathrm{d}s \\ &\le C \Big(\sum_{T \in \mathcal{T}} \eta_2(T, u_\ell)^2 \Big)^{1/2} ||D\Phi_\ell||_{L^2(\Omega)}.\end{aligned}$$

Hölder's inequality implies

$$\int_\Omega Dw_\ell : D\Phi_\ell\,\mathrm{d}x \le \Big(\sum_{T \in \mathcal{T}_k} \eta_2(T, u_k)^2 \Big)^{1/2} ||D\Phi_\ell||_{L^2(\Omega)}.$$

The proof of Theorem 3.9 shows

$$\int_\Omega Du_\ell : D(\phi \times u_\ell)\,\mathrm{d}x \to \int_\Omega D\phi : (u^* \times Du^*)\,\mathrm{d}x.$$

A combination of the assertions with Lemma 3.10 and $||D\Phi_\ell||_{L^2(\Omega)} \le C$ shows that u^* is a harmonic map. $\square$

6. Numerical experiments II

6.1. **Adaptive Algorithm.** Proposition 5.2 motivates the following adaptive mesh refinement algorithm. It realizes uniform mesh-refinement for $\Theta = 0$ and adaptive mesh-refinement for $\Theta = 1/2$. The idea is to iterate steps (b) and (d) of Algorithm (A_h) as long as the energy is significantly decreasing. A termination criterion that may be based on smallness of the local refinement indicators $\eta_j(T, u_h)$ can easily be included.

Algorithm (A_h^Θ)**.** Input: $(\mathcal{T}, u_h^{(0)}, \kappa)$, where $\mathcal{T}$ is a regular triangulation of Ω, $u_h^{(0)} \in \mathcal{A}_h(\mathcal{T}, u_\mathrm{D})$, and $\kappa > 0$.

(a) Set $j := 0$.

- (a1) Solve the optimization problem

$$\begin{cases} \text{Minimize} \quad E(u_h^{(j)} - v_h) \\ \text{subject to} \quad v_h \in \mathcal{S}_0^1(\mathcal{T})^3 \ \text{ and } \ v_h(z) \cdot u_h^{(j)}(z) = 0 \text{ for all } z \in \mathcal{N}. \end{cases}$$

  Denote the solution by $w_h^{(j)}$.
- (a2) Define

$$u_h^{(j+1)} := \sum_{z \in \mathcal{N}} \frac{u_h^{(j)}(z) - w_h^{(j)}(z)}{|u_h^{(j)}(z) - w_h^{(j)}(z)|} \varphi_z.$$

- (a3) If $E(u_h^{(j+1)}) \le E(u_h^{(j)}) - \kappa$ set $j := j + 1$ and go to (a1).

(b) Set $u_h := u_h^{(j)}$.

(c) For each $T \in \mathcal{T}$ compute $\eta(T)^2 := \sum_{j=1}^2 \eta_j(T, u_h)^2$.

(d) Mark all $T \in \mathcal{T}$ which satisfy $\eta(T) \ge \Theta \max_{S \in \mathcal{T}} \eta(S)$ for refinement and generate a new regular triangulation $\mathcal{T}'$ such that all marked elements are refined.

(e) Set $\mathcal{T} := \mathcal{T}'$, construct $u_h^{(0)} \in \mathcal{A}_h(\mathcal{T}, u_\mathrm{D})$ by interpolating nodal values of u_h, and go to (a).

6.2. **Numerical example.** We ran Algorithm (A_h^Θ) with $\Theta = 0$ and $\Theta = 1/2$ in Example 4.1 and an initial triangulation of Ω into 5 tetrahedra. We chose the termination criterion $\kappa := 10^{-4}$ for the iteration in step (a) of Algorithm (A_h^Θ). The mesh refinement was realized by a bisection strategy for $\Theta = 1/2$ and by uniform (red-) refinement for $\Theta = 0$.

The left plot in Figure 7 displays the L^2 error $||u - u_h||_{L^2(\Omega)}$ for uniform and adaptive mesh refinement with the iterates u_h of Algorithm (A_h^Θ). We used a logarithmic scaling on both axes to identify a relation between the number of degrees of freedom and the L^2 error.

We observe that the L^2 error is significantly smaller at comparable numbers of degrees of freedom when the refinement indicators of Proposition 5.2 are used to refine the mesh locally. Moreover, the experimental convergence rate for uniform meshes is only $\mathcal{O}(h)$ (owing to $h = N^{-1/3}$ for uniform meshes) instead of the optimal convergence rate $\mathcal{O}(h^2)$. The adaptive refinement strategy leads to an improved experimental convergence rate. The right plot in Figure 7 displays the discrete energies $E(u_h)$ for uniform and adaptive

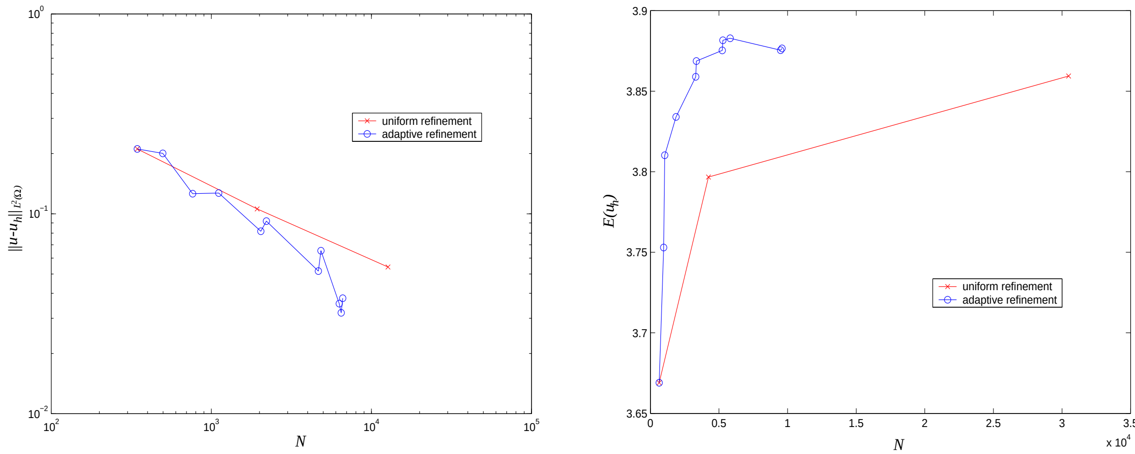

FIGURE 7. L^2 error for uniform and adaptive mesh refinement in Example 4.1 (left). Discrete energies $E(u_h)$ for uniform and adaptive mesh refinement (right).

mesh refinement and we observe that the adaptive strategy reaches a stable value for a smaller number of degrees of freedom than the uniform refinement strategy.

Figure 8 displays the adapted triangulation generated by four iterations of Algorithm $(\mathrm{A}_h^{1/2})$. The dots in the plot indicate the location of a midpoint of a tetrahedron and we observe a refinement towards the origin, where the exact solution has a point singularity.

6.3. **Instability of a degree two singularity.** The final numerical example discusses a situation which leads to more than one degree one singularity.

Example 6.1 ([1, 15])**.** *Let $\pi_s : S^2 \to \mathbb{C}$ denote the stereographic projection of the unit sphere $S^2 \subseteq \mathbb{R}^3$ into the complex numbers $\mathbb{C}$ and given a positive integer p let $\omega(z) := z^p$. Set $\Omega := (-1/2, 1/2)^3$ and $u_{\mathrm{D}}(x) := \pi_s^{-1} \circ \omega \circ \pi_s(x/|x|)$ for $x \in \partial\Omega$.*

We employed Algorithm (A_h^Θ) with $\Theta = 1/2$ in Example 6.1 for $p = 2$ and an initial triangulation of Ω into 5 tetrahedra. We defined an initial function $u_h^{(0)}$ by nodal interpolation of the initial data. Figure 9 displays projections of intermediate solutions restricted to $\{(x, y, 0) : -1/2 \leq x, y \leq 1/2\}$ on the adapted meshes after 0, 4, 8, and 12 iterations of the algorithm. We observe that the initial degree two singularity splits into two degree one singularities and the mesh is refined mostly between the two singularities in which the discrete vector field has a large gradient.

We ran the adaptive algorithm $(\mathrm{A}_h^{1/2})$ in Example 6.1 with $p = 4$ and $p = 8$. The exact solution subject to the corresponding boundary data is expected to have 4 respectively 8 well separated degree one singularities. The projection of the midpoints of the tetrahedra to the plane $\{(x, y, z) \in \mathbb{R}^3 : z = 0\}$ in the left plot of Figure 10 shows that Algorithm $(\mathrm{A}_h^{1/2})$ automatically refines the mesh around four separated points which is in good agreement with the expected behavior of the exact solution. The results for $p = 8$ displayed in the right plot of Figure 10 show a local refinement towards eight points close to the boundary where the separated degree one singularities are expected.

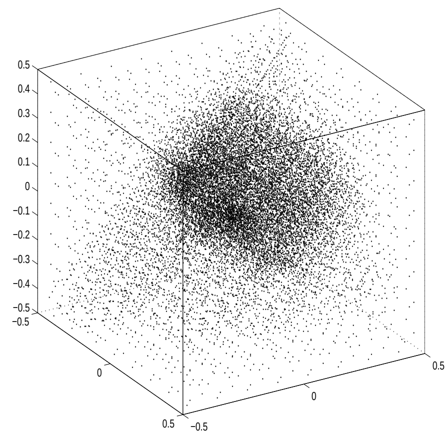

FIGURE 8. Midpoints of tetrahedra (indicated by dots) in the adaptively generated triangulation $\mathcal{T}$ after four iterations of Algorithm $(\mathrm{A}_h^{1/2})$ in Example 4.1.

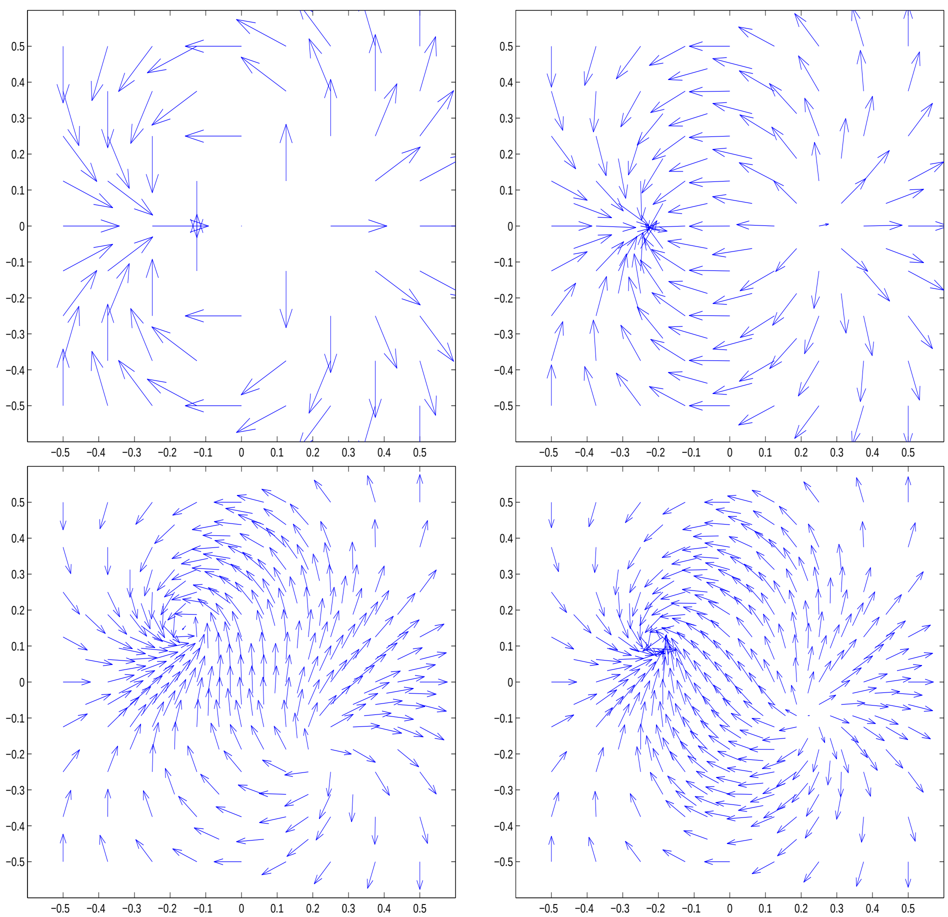

FIGURE 9. Intermediate solutions $u_h(\cdot,\cdot,0)$ in $(-1/2,1/2)^2$ after 0, 4, 8, and 12 iterations of Algorithm $(\mathrm{A}_h^{1/2})$ in Example 6.1.

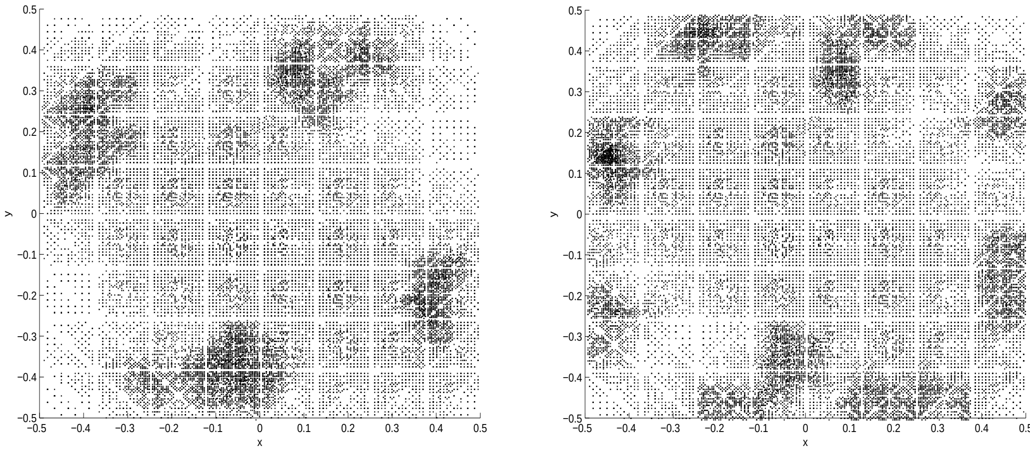

FIGURE 10. Projection of the midpoints of tetrahedra onto the plane $\{(x,y,z) \in \mathbb{R}^3 : z = 0\}$ in Example 6.1 with $p = 4$ (left plot) and $p = 8$ (right plot) after 24 and 18 iterations of Algorithm $(\mathrm{A}_h^{1/2})$, respectively.

Acknowledgments. The author is grateful to one anonymous referee for pointing out the proof of Lemma 3.2. The author is thankful to G.K. Dolzmann and R.H. Nochetto for stimulating discussions. The author wishes to thank J. Bolte for sharing his knowledge on three-dimensional mesh refinement. This work was supported by a fellowship within the Postdoc-Programme of the German Academic Exchange Service (DAAD).

REFERENCES

[1] F. ALOUGES: A new algorithm for computing liquid crystal stable configurations: the harmonic mapping case. *SIAM J. Numer. Anal.* **34**, 1708—1726, 1997.

[2] F. ALOUGES, J.M. GHIDAGLIA: Minimizing Oseen-Frank energy for nematic liquid crystals: algorithms and numerical results. *Ann. Inst. H. Poincaré Phys. Théor.* **66**, 411–447, 1997.

[3] S. BARTELS: Robust a priori error analysis for the approximation of degree-one Ginzburg-Landau vortices. *Preprint*, 2004. Available online at `www.math.umd.edu/~sba`.

[4] S. BARTELS: A posteriori error analysis for time-dependent Ginzburg-Landau type equations. *Numer. Math.* **99**, 557-583, 2005.

[5] J. BEY: Tetrahedral grid refinement. *Computing* **55**, 355-378, 1995.

[6] D. BRAESS: *Finite elements. Theory, fast solvers, and applications in solid mechanics*. 2nd edition. Cambridge University Press, Cambridge, 2001.

[7] H. BREZIS, J.-M. CORON, AND E. LIEB: Harmonic maps with defects. *Comm. Math. Phys.* **107**, 649–705, 1986.

[8] Y. CHEN: The weak solutions to the evolution problem of harmonic maps. *Math. Z.* **201**, 69–74, 1989.

[9] R. COHEN, R. HARDT, D. KINDERLEHRER, S.-Y. LIN, M. LUSKIN: Minimum energy configurations for liquid crystals: Computational results. In *Theory and Applications of Liquid Crystals*, IMA Vol. 5, Springer-Verlag, New York, 99–122, 1987.

[10] R. COHEN, S.-Y. LIN, M. LUSKIN: Relaxation and gradient methods for molecular orientation in liquid crystals. *Comput. Phys. Comm.* **53**, 455–465, 1989.

[11] Q. DU, R. A. NICOLAIDES, X. WU: Analysis and convergence of a covolume approximation of the Ginzburg-Landau model of superconductivity. *SIAM J. Numer. Anal.* **35**, 1049–1072, 1998.

[12] P.-G. DEGENNES, J. PROST: *The Physics of Liquid Crystals*. Clarendon Press, Oxford, 1993.

[13] Q. DU, M. D. GUNZBURGER, J. S. PETERSON: Analysis and approximation of the Ginzburg-Landau model of superconductivity. *SIAM Rev.* **34** (1992), 54–81.

[14] F.C. FRANK: On the theory of liquid crystals. *Discuss. Faraday Soc.* **25**, 19–28, 1958.

[15] R. HARDT, D. KINDERLEHRER, F.-H. LIN: Existence and partial regularity of static liquid crystal configurations. *Comm. Math. Phys.* **105**, 547–570, 1986.

[16] S. HILDEBRANDT, H. KAUL, K.-O. WIDMAN: Dirichlet's boundary value problem for harmonic mappings of Riemannian manifolds. *Math. Z.* **147**, 225–236, 1976.

[17] S. KOROTOV, M. KŘÍŽEK: Acute type refinements of tetrahedral partitions of polyhedral domains. *SIAM J. Numer. Anal.* **39**, 724–733, 2001.

[18] M. KŘÍŽEK, L. QUN: On diagonal dominance of stiffness matrices in 3D. *East-West J. Numer. Math.* **3**, 59–69, 1995.

[19] H.W. KUHN: Some combinatorial lemmas in topology. *IBM J. Res. Develop.* **4**, 508–524, 1960.

[20] F.-H. LIN: A remark about the map $x/|x|$. *C. R. Acad. Sci. Paris* **305**, 529–531, 1987.

[21] S.-Y. LIN, M. LUSKIN: Relaxation methods for liquid crystal problems. *SIAM J. Numer. Anal.* **26**, 1310–1326, 1989.

[22] C. LIU, N.J. WALKINGTON: Approximation of liquid crystal flows. *SIAM J. Numer. Anal.* **37**, 725–741, 2002.

[23] C. LIU, N.J. WALKINGTON: Mixed methods for the approximation of liquid crystal flows. *M2AN Math. Model. Numer. Anal.* **36**, 205–222, 2002.

[24] C. W. OSEEN: The theory of liquid crystals. *Trans. Faraday Soc.* **29**, 883–899, 1933.

[25] A. PROHL: *Computational micromagnetism.* Advances in Numerical Mathematics. B. G. Teubner, Stuttgart, 2001.

[26] M. RENARDY, R.C. ROGERS: *An introduction to partial differential equations.* Texts in Applied Mathematics, Springer-Verlag, New York, 1993.

[27] T. RIVIÈRE: Existence of infinitely many weakly harmonic maps into spheres for non constant boundary datas. *Preprint 9419, Centre de Mathématiques et de Leurs Applications*, Cachan, France, 1994.

[28] T. RIVIÈRE: Everywhere discontinuous harmonic maps into spheres. *Acta Math.* **175** 197–226, 1995.

[29] R. SCHOEN, K. UHLENBECK: A regularity theory for harmonic maps. *J. Differential Geom.* **17**, 307–335, 1982.

[30] M. STRUWE: On the evolution of harmonic mappings of Riemannian surfaces. *Comment. Math. Helv.* **60**, 558–581, 1985.

[31] E.G. VIRGA: *Variational theories for liquid crystals.* Applied Mathematics and Mathematical Computation, 8. Chapman & Hall, London, 1994.